Journal of Radioanalytical and Nuclear Chemistry
https://doi.org/10.1007/s10967-023-09308-2

Towards a re-determination of the ^{42}Ar half-life

D. Schumann[1] · E. Maugeri[1] · Y. Dai[1] · R. Dressler[1] · U. Köster[2]

Received: 25 September 2023 / Accepted: 2 December 2023

Abstract
We report on a new measurement of the half-life of ^{42}Ar by following its decay over a time period of more than 13 years using γ-ray spectrometry. The obtained value of (39.5 ± 3.6) y confirms the only other, previously measured value of (33 ± 2) y. However, since partial outgassing of the accumulated Ar from the sample cannot be excluded, this value should be understood as a lower limit. The sample has now been stored in a gas-tight quartz ampoule to enable further measurements excluding the outgas effect in order to confirm our finding.

Keywords Half-life · Argon-42 · Decay data · γ-ray spectrometry · Isotope production

Introduction

^{42}Ar is produced in the geosphere by bombardment of rocks with cosmic rays and in the Earth atmosphere via the ^{40}Ar(α; 2p) reaction as well as by double neutron capture on ^{40}Ar [17]. Part of the currently present ^{42}Ar in the atmosphere can probably also originate from nuclear bomb tests during the years from 1945–1962 [5]. The content of ^{42}Ar in natural Ar poses a significant background problem in experiments seeking to measure the half-life of neutrinoless double-beta decay [2, 17]. Especially the daughter decay of ^{42}K is a dominant background in experiments like GERDA (https://www.mpi-hd.mpg.de/gerda/) and LEGEND (https://legend-exp.org/) that are using liquid argon as veto. The concentration of ^{42}Ar in atmospheric argon is not well determined, there are several, partly contradictory measurements [1–4, 6]. To assess the situation, especially if long-term experiments are planned, the decay rate of ^{42}Ar is important in addition to knowing its production routes and rates. However, data on the half-lives of longer-lived radionuclides are often insufficient and/or uncertain [10], and this is unfortunately also true for ^{42}Ar.

An early estimate is given by Katcoff [11] in 1952 as a lower limit of 3.5 years and by Stoenner et al. in 1960 [15] as ~ 30 y. The currently adopted value of Nuclear Data Sheets [8] is (32.9 ± 1.1) y, which is based on only one measurement performed also by Stoenner et al. in 1965 [16]. In the mentioned work, the half-lives of ^{37}Ar, ^{39}Ar, and ^{42}Ar were determined simultaneously by applying β- and γ-spectrometry to measure the activity, as well as mass spectrometry to deduce the number of atoms. The half-life of ^{37}Ar ($t_{1/2}$ = (35.14 ± 0.05) d [16]) was determined following the decay, while for ^{39}Ar and ^{42}Ar the formula $t_{1/2} = N \cdot \ln 2 / A$ was used (here N denotes the number of atoms in the sample, whereas A is its activity), and the half-lives were calculated relatively to the ^{37}Ar half-life. The advantage of this approach was that for the latter two only the isotope and activity ratios had to be determined and no absolute measurements were required. Note that, in contrast to the 3% uncertainty reported in [16], the authors additionally took into account possible systematic errors in mass spectrometry, sample transfer and counter efficiency measurements, leading finally to an estimated uncertainty of 6%, thus a value of (33 ± 2) y will be adopted here. In view of the above mentioned importance of the isotope and the fact that there is only one experimental determination so far, a new measurement of the half-life of ^{42}Ar is highly desirable.

✉ D. Schumann
dorothea.schumann@psi.ch

[1] Division of Nuclear Energy and Safety, Paul Scherrer Institute, Forschungsstrasse 111, 5232 Villigen, Switzerland

[2] Institut Laue-Langevin, Grenoble, France

Published online: 09 January 2024

Experimental

Sample description

Besides the production routes described above, an alternative possibility for producing ^{42}Ar is spallation induced by high-energy protons or neutrons on targets with higher mass. For the envisaged half-life determination, Ti samples were available which had been irradiated together with five other samples for two years in the target of the SINQ facility at PSI in the frame of the STIP IV program [9]. The initial aim of the irradiation of these special specimens was the production of exotic radionuclides for scientific research purposes in nuclear astrophysics (for instance ^{60}Fe, ^{54}Mn, ^{59}Ni produced by proton and neutron irradiation in Cu) as well as for the development of new radiopharmaceuticals (e.g. ^{44}Ti produced by proton and neutron irradiation in Ti). Figure 1 shows a photo of these 6 specimens irradiated in STIP IV, with the sample used for the present half-life determination of ^{42}Ar being No. 4 (dimensions 1 mm × 3 mm × 6 mm). The irradiation was performed from April 29th, 2004 until December 22nd, 2005. During a total of 17 months of operation, the entire SINQ target received a proton charge of 10.87 Ah with an average proton energy of 575 MeV [9]. After a cooling time of 5 years, the specimens were removed from the target assembly in spring 2010.

γ-ray measurements

Three different high purity single-crystal Ge (HPGe) detectors were used for the measurements: The initial measurement was performed on 16.03.2010 with a coaxial P-type HPGe detector (detector 1: EGPC 12, Canberra) with a crystal of 47 mm diameter and 54 mm thickness (FWHM at 122, 0.96 and at 1332, 1.96 keV). The intermediate measurement was performed on 09.12.2022 using a coaxial N-type HPGe detector (detector 2: EGNC 15, EURISYS) with a crystal of 49 mm diameter and 45 mm thickness (FWHM at 122, 0.82 keV and at 1332, 1.85 keV). The so far last measurements were performed in July 2023 using a broad energy Ge detector (detector 3: BEGe 2825, Mirion Tech.—Canberra) with a crystal of 61 mm diameter and 26 mm thickness (FWHM at 122, 0.60 keV and at 1332, 1.68 keV). The GENIE2000 (Mirion Tech.—Canberra) software was used for the data acquisition and analysis. The energy calibrations were performed using a standard ^{152}Eu calibration source.

Fig. 1 Photo of the six samples (1–4: Ti; 5 and 6: Cu) before irradiation inside the SINQ target at PSI in the frame of the STIP IV material investigation program. Sample No. 4 served for the half-life determination of ^{42}Ar

Half-life determination approach

Besides the above mentioned method, which exploits the equation $t_{1/2} = N \cdot \ln 2 / A$, e.g. applied in [16], a decay rate measurement following the change of the activity in a sample can also be considered suitable, if the targeted half-life is reasonable small and provided that a sample being stable over a time period of several years is available. Since the decay product of ^{42}Ar is ^{42}K with a half-life of $t_{1/2} = (12.355 \pm 0.007)$ h [8], the system is in secular equilibrium after a comparably short time after production and thus, the radioactive decay of ^{42}Ar can be followed by measuring the intensity of the ^{42}K γ line at 1525 keV. Some other isotopes with well-determined half-lives are present in the sample and are used as internal reference for the half-life determination of ^{42}Ar. These are ^{22}Na ($t_{1/2} = (2.6019 \pm 0.0006)$ y [12]) with a characteristic γ line at 1275 keV, ^{60}Co ($t_{1/2} = (5.2714 \pm 0.0006)$ y [12]) with two characteristic γ lines at 1173 keV (intensity 99.85% ± 0.03%) and at 1332 keV (intensity 99.9826 ± 0.0006%), and ^{44}Ti ($t_{1/2} = (59.1 \pm 0.3)$ y [12]) that is in secular equilibrium with its daughter ^{44}Sc ($t_{1/2} = (4.0421 \pm 0.0025)$ h [12]). The latter emits a γ line at 1157 keV (intensity 99.90 ± 0.42%) and, weaker, at 1499 keV (intensity 0.908 ± 0.015%). Because of the high activity of the sample resulting in a dose rate on contact of about 1 mSv/h, all measurements were performed at reasonably large distances of around 1 m to keep the counting dead time well below 10%. Consequently, no reliable full energy peak efficiency (FEPE) calibrations could be performed with certified sources available at PSI. Thus, the ^{42}Ar half-life was deduced by comparing the count rate ratios of the ^{42}K γ line and the γ lines of reference nuclides between the initial measurement in 2010 and the follow-up measurements till 2023.

A general characteristics of HPGe detectors is the pronounced power-law behavior for the FEPE above 500 keV (see Fig. 2 for measured FEPE of detector 3). Thus the FEPE can be expressed in this region as

$$\varepsilon(E) = \alpha \times E^{\beta} \tag{1}$$

where ε is the value of the FEPE at the energy E, the pre-exponential parameter α and the exponential coefficient β depends on the particular dimensions of the Ge single-crystal as well as on the used measurement geometry. The pre-exponential parameter α will affect all FEPE in the same manner thus the FEPE value at the energy of the ^{42}K γ line

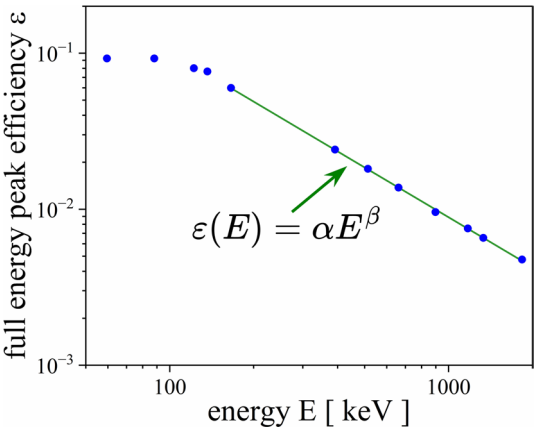

Fig. 2 Measured full energy peak efficiency of detector 3. The blue data points represent measured values (uncertainties are smaller as the symbol size). In addition, the general power law behavior of the FEPE for higher photon energies is plotted as green line

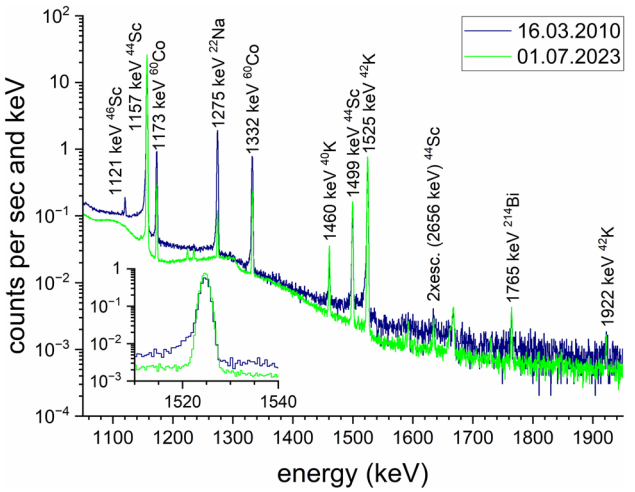

Fig. 3 Part of the γ-ray spectrum of sample No. 4 over the relevant energy region performed with detector 1 and detector 3. The magnified inset of the 1525 keV ^{42}K γ line demonstrates the different lineshapes of the HPGe detectors used in the measurement of 2010 and 2023, respectively

at 1525 keV is used as normalization point. The power coefficient β is calculated using the peak areas P_1 and P_2 of the two prominent ^{60}Co γ lines at $E_1 = 1173$ keV and $E_2 = 1332$ keV by

$$\beta = \frac{\ln(P_1) - \ln(P_2)}{E_2 - E_1} \tag{2}$$

with its uncertainty uβ

$$u\beta^2 = \left\{ \left(\frac{uP_1}{P_1} \right)^2 + \left(\frac{uP_2}{P_2} \right)^2 \right\} \times \left(\frac{1}{E_2 - E_1} \right)^2 \tag{3}$$

where uP_1 and uP_2 denotes the uncertainties of P_1 and P_2, respectively.

Therefore, the change in the FEPE for all energies of the used γ lines can be accounted using a relative FEPE transfer with respect to the FEPE of the ^{42}K γ line at 1525 keV in the very same measurement.

This approach allows the determination of the half-life without detailed knowledge of the absolute FEPE by solely using the peak area ratios of two corresponding γ lines. The uncertainty budget in our measurements is dominated by the uncertainties of the relative FEPE transfer and in minor extent by the counting statistics.

Results and discussion

The first γ-ray measurement of sample No. 4 was performed on 16.03.2010 using detector 1. This measurement was performed with the original aim to get a rough overview on the amounts of the main produced isotopes, in particular of ^{44}Ti, in order to evaluate the feasibility of the production route for medically applicable purposes and to obtain enough sample material for the development of a prototype ^{44}Ti/^{44}Sc generator system. The later on envisaged usage of such samples for the half-life determination of ^{42}Ar was not in the focus at that time. After the measurement, the samples had been stored in the storage of the PSI Hotlab for 13 years. A second measurement was performed on 09.12.2022 using detector 2 after the sample was retrieved from the dry storage. The so far last measurements were performed in July 2023 using detector 3. In Fig. 3, the γ-ray spectra of initial measurements at 16.03.2010 and the last follow-up measurements at 01.07.2023 are shown.

Besides the isotope of interest, ^{42}Ar, detected using the γ line of its short-lived daughter ^{42}K, ^{44}Ti and its short-lived daughter ^{44}Sc were identified as the main reaction products. Additionally, ^{22}Na, ^{46}Sc, ^{54}Mn and $^{57/60}$Co were detected. The origin of these isotopes is either a by-product from spallation of Ti or a cross-contamination from spallation of Cu samples – irradiated and stored together with the Ti-samples, or some higher mass impurities contained in the Ti samples respectively.

In Table 1, the peak areas of the ^{22}Na γ line at 1275 keV, the ^{44}Sc γ lines at 1157 keV and 1499 keV (attributed to ^{44}Ti), and the ^{42}K γ line at 1525 keV (attributed to ^{42}Ar) are summarized for all measurements. The results of the performance check of the here used method reproducing the well-known half-lives of ^{22}Na, ^{44}Ti, ^{60}Co are summarized in Table 2.

The ^{42}Ar half-life can be calculated using the equation

Table 1 Peak areas of the used reference isotope and the 1525 keV γ lines of sample No. 4, measured on 16.03.2010, 01.07.2023, and 25.07.2023, respectively, as well as the deduced values of the ^{42}Ar half-life

	Reference isotope and used γ line					
	^{22}Na 1275 keV	^{60}Co 1173 keV	^{60}Co 1332 keV	^{44}Ti 1157 keV	^{44}Ti 1499 keV	^{42}Ar 1525 keV
Peak areas 16.03.2010	70,770 ± 298	32,860 ± 239	29,390 ± 194	605,600 ± 815	4317 ± 81	22,690 ± 160
Relative FEPE	1.172 ± 0.016	1.262 ± 0.025	1.127 ± 0.012	1.277 ± 0.027	1.0149 ± 0.0013	**1**
Peak areas 09.12.2022	30,620 ± 204	78,210 ± 948	69,520 ± 727	6,731,000 ± 4990	46,480 ± 545	225,400 ± 946
Relative FEPE	1.183 ± 0.027	1.278 ± 0.042	1.134 ± 0.019	1.295 ± 0.045	1.0157 ± 0.0021	**1**
Deduced ^{42}Ar half-life	32.0 ± 3.3	36.07 ± 0.48	36.069 ± 0.063	35.68 ± 0.13	38.64 ± 0.13	
Peak areas 01.07.2023	26,470 ± 372	72,030 ± 383	63,490 ± 340	6,843,000 ± 2665	48,270 ± 251	231,800 ± 497
Relative FEPE	1.197 ± 0.013	1.300 ± 0.020	1.1446 ± 0.0092	1.319 ± 0.022	1.0168 ± 0.0010	**1**
Deduced ^{42}Ar half-life	36.6 ± 3.4	47.78 ± 0.22	47.777 ± 0.094	40.948 ± 0.081	38.6021 ± 0.0042	
Peak areas 25.07.2023	82,110 ± 597	222,700 ± 662	197,600 ± 605	21,660,000 ± 4701	152,700 ± 432	734,400 ± 873
Relative FEPE	1.1856 ± 0.0071	1.283 ± 0.011	1.1365 ± 0.0051	1.300 ± 0.012	1.01593 ± 0.00057	**1**
Deduced ^{42}Ar half-life in years	37.6 ± 2.8	48.861 ± 0.076	48.861 ± 0.032	38.816 ± 0.023	37.9940 ± 0.0013	

Table 2 Performance check of the used method

Isotope γ line adopted half-life	Reference isotope			
	^{22}Na	^{44}Ti	^{60}Co	Overall mean
^{22}Na 1274.6 keV (2.6019 ± 0.0006) y		(2.657 ± 0.027) y −2.1%	(2.25 ± 0.23) y −13%	(2.44 ± 0.13) y −6.3%
^{44}Ti 1157.0 keV (59.1 ± 0.3) y	(52.0 ± 2.7) y −12%		(72.0 ± 5.3) y +22%	(63.8 ± 4.5) y +7.9%
^{60}Co 1173.3 keV (5.2714 ± 0.0006) y	(5.127 ± 0.032) y −2.7%	(5.189 ± 0.064) y −1.6%		(5.168 ± 0.025) y −2.0%

Given are the deduced half-lives and their uncertainties of ^{22}Na, ^{44}Ti, and ^{60}Co using the respective two other isotopes together with the relative deviation in percent from the adopted half-life values, which are quoted in the column heads (all taken from [12]). In addition the overall means are presented, for which the data of all obtained γ-ray spectra are used

$$\lambda_{Ar,j,i} = \lambda_j + \frac{1}{\Delta t_i} \ln\left(\frac{\varpi_{j,i}/\varpi_{Ar,i}}{\varpi_{j,0}/\varpi_{Ar,0}}\right) \tag{4}$$

$\lambda_{Ar,j,i}$ decay constant ^{42}Ar deduced from the j-th reference isotope and in the i-th follow-up measurement

λ_j decay constant of the j-th used reference isotope

Δt_i time between initial and i-th follow-up measurement

$P_{j,i}$ peak area of the j-th γ lines in the i-th measurement

$\varepsilon_{j,i}$ relative FEPE of the j-th γ lines in the i-th measurement

$\varpi_{j,i}$ relative FEPE corrected peak area of the j-th γ lines in the i-th measurement according to:

$$\varpi_{j,i} = \frac{P_{j,i}}{\varepsilon_{j,i}}$$

Herein the indices j and i refer to the isotopes and measurements, respectively. Especially, $j=0$ refers to the γ line of ^{42}K and $i=0$ to the initial measurement on 16.03.2010. In total $M=5$ different γ lines in $N=3$ follow-up measurement were used.

The overall mean of all deduced.^{42}Ar half-life values was calculated using the following formula Eq. (5)

$$\lambda_{Ar} = \frac{\sum_{j,i}\lambda_{\mathrm{Ar},j,i}}{M\cdot N} = \frac{1}{M}\sum_{j=1}^{M}\lambda_j + \frac{1}{N}\sum_{i=1}^{N}\frac{1}{\Delta t_i}\cdot\left\{\ln \nu_{\mathrm{Ar},0} - \frac{1}{M}\sum_{j=1}^{M}\ln \nu_{j,0}\right\} - \frac{1}{N}\sum_{i=1}^{N}\frac{1}{\Delta t_i}\left\{\ln \nu_{\mathrm{Ar},i} - \frac{1}{M}\sum_{j=1}^{M}\ln \nu_{j,i}\right\} \tag{5}$$

The combined standard uncertainty $\upsilon\lambda_{\mathrm{Ar}}$ with a coverage factor $k=1$ consists of two parts, an intrinsic uncertainty $\upsilon\lambda_{\mathrm{int}}$ representing the standard error of the used data and an extrinsic uncertainty $\upsilon\lambda_{\mathrm{ext}}$ deduced by Gaussian error propagation of Eq. (5) as

$$\upsilon\lambda_{\mathrm{Ar}}^2 = \upsilon\lambda_{\mathrm{int}}^2 + \upsilon\lambda_{\mathrm{ext}}^2 \tag{6}$$

Table 3 Uncertainty budget for the overall mean of the ^{42}Ar half-life

Type of uncertainty	Absolute uncertainty	Relative uncertainty (%)	Partial contribution (%)
Extrinsic			
^{22}Na, ^{44}Ti, ^{60}Co half-life	0.048 y	0.12	0.018
^{60}Co branching	0.074 y	0.19	0.043
FEPE transfer initial meas	1.2 y	2.9	10
FEPE transfer follow-up meas	2.3 y	5.8	40
Peak areas initial meas	1.4 y	3.6	15
Peak areas follow-up meas	1.0 y	2.7	8.6
Tailing of peak areas initial meas	1.2 y	3	11
Intrinsic			
Statistical variations	1.4 y	3.4	14
Total	3.6 y	9.1	100

This ensures a conservative estimate of the combined uncertainty that does not more than 41% exceed the true value.

Using these formulas the overall mean ^{42}Ar of the half-life is deduced to be $t_{1/2} = (39.5 \pm 3.6)$ y. The detailed uncertainty budget is given in Table 3.

Our experimentally determined value is consistent with the value reported in [16]. However, the determination presented here faces a few challenges.

- The six samples had not been individually sealed in airtight vessels, but were stored together in an aluminum box in the dry storage of the Hotlab at PSI till December 2022. Therefore, it cannot be ruled out that part of the Ar has outgassed during the storage period. This, in turn, would result in a shorter half-life value than the true half-life.
- Three different detectors have been used for the measurements, which showed clear differences in the energy dependence of the full energy peak efficiency.
- Since only an overview measurement was planned in 2010, too little attention was paid to the detector performance, which caused a peak shape that was not ideal (see inset of Fig. 3). Due to the appearing low-energy tailing, the peaks had to be fitted manually using the interactive peak fit tool. The resulting uncertainty was estimated to additional 3%.

In particular, a possible outgassing could lead to uncontrolled losses, which would result in an apparently accelerated decay.

No literature values are available for room temperature diffusion of argon in titanium metal. However, an indirect estimate can be made via the diffusion coefficients of other impurity atoms in titanium. It has been shown that diffusivity is inversely related to the atomic/ionic radius of the diffusing species [13]. Extrapolating the Arrhenius plots of potassium (diffusing as K^+ with 138 pm effective ion radius) and calcium (diffusing as Ca^{2+} with 100 pm ion radius) [7] to 500°C leads to diffusivities of $\approx 3 \times 10^{-21}$ m^2/s and $\approx 4 \times 10^{-23}$ m^2/s respectively. Argon (diffusing as neutral Ar^0 with 200 pm van der Waals radius) would have even much lower diffusivities. Assuming a diffusivity of 3×10^{-21} m^2/s the solution of Fick's second law for a 1 mm thick foil leads to only 0.25% diffusion release after 13 years. The extrapolated diffusion release of argon at room temperature is still far lower, i.e. diffusional release from Ti metal is not expected to affect the measurement significantly. However, the diffusion data from literature were obtained by radiotracer measurements of Ti foils irradiated at low dose. The high dose irradiation of our sample could have led to significant radiation damage and/or radiation-enhanced oxidation of the surface layer of the Ti sample. Either could affect the diffusivity in an unpredictable manner. Therefore, the preliminary half-life value given here has to be understood as a lower limit of the true half-life. Notwithstanding these shortcomings of the here present result, this is consistent with the in [16] reported half-life and consequently can be considered as a valuable indication that the reported value is correct. Indirectly, this also increases the confidence in the accuracy of the half-life for ^{39}Ar, which had been determined by the same authors in the same experiment. There is only one earlier half-life determination of ^{39}Ar (265 ± 30) y by Zeldes et al. [18], which is in perfect agreement with the value reported in [16], albeit with a factor of 10 higher uncertainty. Our implicit confirmation is of special importance, because ^{39}Ar is considered as one of the rare possible tools for nuclear dating of environmental samples from the period of early industrialization (100–1000 years) [18], similar to ^{32}Si described in [18].

Conclusions and outlook

To definitively exclude any further Ar release, we sealed the sample in a quartz ampoule (Fig. 4) and will repeat γ-ray measurements during the next decades. The data analysis and evaluation should then also include peak area ratios

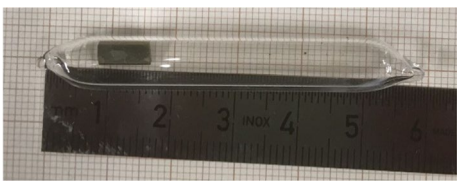

Fig. 4 Photo of sample No. 4 (irradiated Ti), sealed in a quartz ampoule

obtained using by analyzing all possible peak areas of ^{22}Na, ^{44}Ti, and ^{60}Co γ lines.

An additional advantage would be that the peak shapes of the relevant peaks in the measured spectra are then well under control.

Funding Open Access funding provided by Lib4RI – Library for the Research Institutes within the ETH Domain: Eawag, Empa, PSI & WSL.

Declarations

Conflict of interest The authors declare not to have any conflicts of interests.

References

1. Agostini M (2014) The background in the 0νββ experiment GERDA. https://doi.org/10.1140/epjc/s10052-014-2764-z
2. Ajaj R (2019) Electromagnetic backgrounds and potassium-42 activity in the DEAP-3600 dark matter detector. https://doi.org/10.1103/PhysRevD.100.072009
3. Ashitkov VD (1998) New experimental limit on the ^{42}Ar content in the Earth's atmosphere. https://doi.org/10.1016/S0168-9002(98)00740-2
4. Ashitkov VD (2003) A liquid-argon ionization detector for the study of double beta decay. Instruments Exp Techn. https://doi.org/10.1023/A:1023605413765
5. Barabash AS (1997) Estimate of the ^{42}Ar content in the earth's atmosphere. Nuclear Instruments Methods Phys Res. https://doi.org/10.1016/S0168-9002(96)01074-1
6. Barabash AS (2016) On concentration of ^{42}Ar in the Earth's atmosphere. Nuclear Instruments Methods Phys Res. https://doi.org/10.1016/j.nima.2016.09.042ts
7. Beyer GJ (2003). The role of diffusion in ISOL targets for the production of radioactive ion beams. https://doi.org/10.1016/S0168-583X(02)01913-4
8. Chen J (2016) Nuclear Data Sheets for A=42. https://doi.org/10.1016/j.nds.2016.06.001
9. Dai Y (2012) The fourth SINQ Target Irradiation program. STIP-IV. https://doi.org/10.1016/j.jnucmat.2011.11.004
10. Heinitz S (2022) How accurate are half-life data of long-lived radionuclides?. https://doi.org/10.1515/ract-2021-1135
11. Katcoff S (1952) Thermal neutron capture cross section of ^{40}Ar and observation of ^{42}Ar. https://doi.org/10.1103/PhysRev.87.886
12. Kondev FG (2020) The NUBASE2020 evaluation of nuclear physics properties. https://doi.org/10.1088/1674-1137/abddae
13. Nakajima H (1991) Diffusion in titanium. ISIJ Int. https://doi.org/10.2355/isijinternational.31.757
14. Stoenner RW (1960). Meteorites as space probes for testing the spatial constancy of cosmic radiation. J Geophys Res. https://doi.org/10.1029/JZ065i010p03025
15. Stoenner RW (1965) Half-lives of Argon-37, Argon-39, and Argon-42. https://doi.org/10.1126/science.148.3675.1325
16. Veicht M (2021) Radiochemical separation and purification of non-carrier-added silicon-32. https://doi.org/10.1515/ract-2021-1070
17. Zang C (2022) Evaluation of cosmogenic production of ^{39}Ar and ^{42}Ar for rare-event physics using underground argon. https://doi.org/10.1016/j.astropartphys.2022.102733
18. Zeldes H (1952) Half-life and mass assignment of Argon 39. https://doi.org/10.1103/PhysRev.86.811